

Electronic structure and spin polarization of Mn-containing dilute magnetic III-V semiconductors

Manish Jain, Leeor Kronik, and James R. Chelikowsky

Department of Chemical Engineering and Materials Science, and Minnesota Supercomputing Institute, University of Minnesota, Minneapolis, Minnesota 55455

Vitaliy V. Godlevsky

Department of Physics and Astronomy, Rutgers University, Piscataway, New Jersey 08854

(Received 16 February 2001; revised manuscript received 22 June 2001; published 3 December 2001)

We present *ab initio* density-functional calculations for the electronic structure of the dilute magnetic semiconductors $\text{Mn}_x\text{Ga}_{1-x}\text{As}$ and $\text{Mn}_x\text{In}_{1-x}\text{As}$ with a realistic $x=0.063$. We find that the introduction of Mn perturbs the position of the nearest As atoms, but does not break the tetrahedral symmetry. Neither material is found to be strictly half metallic. However, in both materials the Mn content results in a majority-spin valence-band maximum that is ~ 0.5 eV above the minority-spin valence-band maximum. This large valence-band split is primarily due to the hybridization of As $4p$ and Mn $3d$ orbitals. It results in a significant energy range where holes have a well-defined spin. The effective masses of holes in this range are found to be comparable to those of GaAs and InAs. Hence, in an ideal, disorder-free situation, spin-polarized transport may be explained by conventional transport in the context of a simple band picture. This leads to a theoretical limit of 100% spin injection from these materials. Attaining this limit in a sufficiently ordered material also requires a careful “engineering” of the Fermi-level position and a sufficiently low temperature.

DOI: 10.1103/PhysRevB.64.245205

PACS number(s): 71.20.Nr, 71.55.Eq, 75.50.Pp

I. INTRODUCTION

The systematic use of electron *spin*, in addition to its *charge*, holds great promise for a new class of semiconductor devices with unprecedented functionality. The suggested applications include, e.g., “spin-field-effect transistors”¹ which could allow for software re-programming of the microprocessor hardware during run time, semiconductor-based “spin-valves”² which would result in high-density, non-volatile semiconductor memory chips, and even “spin qubits”³, to be used as the basic building block for quantum computing.

A major hindrance for the practical implementation of the above concepts is the difficulty in preparing materials that can serve as a high-efficiency source of charge carriers with well-defined spin, yet be compatible with existing semiconductor technologies. For example, it has been theoretically shown that the ferromagnetic zinc-blende phase of MnAs (that could, in principle, be compatible with GaAs), is half metallic,⁴ i.e., the majority-spin states have a metallic density of states and the minority-spin states have a semiconducting density of states, with the Fermi level lying in the semiconducting gap. Electrons injected from the vicinity of the Fermi level would have well-defined spins, making zinc-blende MnAs ideally suited for spin-injection applications. Unfortunately, this phase has yet to be grown successfully, and indeed subsequent theoretical work has shown that it cannot be stabilized at equilibrium.⁵

Recently, significant progress in the growth of dilute magnetic semiconductors (DMSs) has been reported.⁶ This breakthrough was made possible by using nonequilibrium molecular-beam epitaxy growth for incorporating Mn in excess of the solubility limit into III-V semiconductors, most notably GaAs (as much as $\sim 8\%$ Mn) and InAs (as much as $\sim 17\%$ Mn).⁶ Clearly, these new compounds are compatible

with existing III-V semiconductor technology. Some initial success in using them for injecting spin-polarized holes has been reported recently,^{7,8} albeit with a limited degree of spin polarization (several percent). High-efficiency spin injection from these materials remains a formidable task.

Here, we examine the theoretical limits to spin injection from dilute III-V magnetic semiconductors by using first-principles calculations, based on spin-polarized density-functional theory. We compute the electronic structure of the ferromagnetic ordered phase of $\text{Mn}_x\text{Ga}_{1-x}\text{As}$ and $\text{Mn}_x\text{In}_{1-x}\text{As}$, with $x=0.063$ (i.e., in the experimentally relevant range), and find that ideal (fully polarized) spin injection is indeed *possible*. This is because the introduction of Mn results in a significant energy range (~ 0.5 eV) where holes have a well-defined spin. Hole mobility is then explained on the basis of a simple band-transport picture, which facilitates the ideal limit of spin-polarized transport. In light of these findings, we discuss the stringent conditions on the band lineup at the DMS/semiconductor interface that are required for a practical utilization of this hole band.

II. COMPUTATIONAL DETAILS

All calculations presented below were performed by using *ab initio* pseudopotentials within density-functional theory, with a plane-wave basis.⁹ We employed the local-spin-density approximation, implemented using the Perdew-Wang exchange-correlation functional,¹⁰ and used Troullier-Martins pseudopotentials¹¹ cast into the separable Kleinman-Bylander form.¹² Pseudopotentials based on electronic configurations of $4s^{1.75}4p^{0.25}3d^5$ (Mn), $4s^24p^14d^0$ (Ga), $5s^25p^15d^0$ (In), and $4s^24p^34d^0$ (As), with *s/p/d* cutoff radii (in atomic units) of 1.90/2.59/2.00, 2.99/2.58/2.99, 3.00/3.00/3.00, and 2.49/2.49/2.49, respectively, were used. A plane-wave cutoff energy of 60 Ry and a Monkhorst-Pack¹³

$4 \times 4 \times 4$ k -point sampling scheme were used to guarantee convergence.

All DMS calculations were performed within a 32-atom supercell, constructed as follows. By taking $2 \times 2 \times 2$ standard unit cells of the zinc-blende structure, we constructed the ideal GaAs or InAs lattice as a simple cubic lattice of supercells containing 64 atoms. We then transformed this lattice into an equivalent body-centered-cubic (bcc) lattice of supercells containing 32 atoms. Finally, we replaced one Ga or In atom with a Mn atom, obtaining a DMS with $\sim 6.3\%$ of MnAs (i.e., $x=0.063$). Because the supercell contains only one Mn atom and the infinite crystal is constructed by exact replications of this supercell, all Mn atoms have the same neighboring atoms and possess the same spin. Therefore, the MnGaAs or MnInAs phase so constructed is *ferromagnetic and ordered* by definition.

Partial density-of-states curves were computed by using a sphere of ~ 1.3 Å (which is close to the covalent radius of all atomic species involved), centered on each atom, to deconvolve the obtained wave functions over atomic orbitals of valence electrons. The resulting density of states was only weakly dependent on the radius chosen, within a range of several tenths of angstroms around this radius. The same sphere size was used for calculating local magnetic moments.

III. STRUCTURAL OPTIMIZATION

The introduction of a Mn impurity into the GaAs or InAs matrix is expected to disrupt the local atomic structure around the impurity. This disruption may alter the electronic structure significantly, especially if it is associated with symmetry lowering. We therefore initiated our study by calculating the equilibrium atomic positions in the supercell, as a prerequisite in calculating the electronic structure. To that end, we have perturbed all atoms from their original positions in the supercell, so as to destroy any remaining formal symmetry. We then allowed each atom to move under the forces exerted by the electrons and the other atoms and minimized the total energy using the Broyden-Fletcher-Goldfarb-Shanno algorithm¹⁴ to find the new atomic equilibrium positions.

For both materials, we find that the introduction of Mn has a non-negligible effect only on the position of its first As neighbors, where the cation-As bond length is altered, but the tetrahedral symmetry is maintained. Subsequent shells are left unperturbed. Our findings are in good agreement with experiment. For MnGaAs, we find the Mn-As bond to be slightly elongated with respect to the Ga-As one (2.48 Å vs 2.44 Å, respectively), whereas for MnInAs, the Mn-As bond is slightly compressed with respect to the In-As one (2.51 Å vs 2.62 Å, respectively). This is simply because the Mn-As bond length in MnAs, 2.57 Å, is longer than that of Ga-As in GaAs but shorter than that of In-As in InAs.¹⁷ Moreover, the computed Mn-As bond lengths are in good agreement with those found experimentally [2.50 Å (Refs. 17) and 2.54–2.58 Å (Ref. 18) for MnGaAs and MnInAs, respectively], using extended x-ray-absorption fine structure measurements of samples with a comparable Mn fraction. In

both cases, the calculated value slightly underestimates the experimental value—a well-known result of the local-density approximation.⁵ We note that for MnGaAs, a Mn-induced static disorder of the first Ga shell and second As shell was also reported.¹⁷ This disorder was not reproduced in our calculations. However, we do not expect the introduction of an ordered array of impurities into an ordered lattice to introduce a disorder (unlike a *reduced* degree of order, i.e., symmetry lowering, which is possible). We, therefore, attribute the observed disorder to the alloy disorder of the Mn atoms in a real MnGaAs sample, as opposed to the perfect ordering of Mn in our computed alloy.

All electronic structure calculations shown below were performed using the above-discussed optimized geometry. However, because the Mn-induced perturbation maintained the tetrahedral symmetry and was quantitatively small, we find that its effect on the electronic structure is negligible. This constitutes a *first-principles* support for the neglect of structural effects in computing the electronic structure of these materials, previously used as an *ansatz*.^{4,15,16}

IV. MAGNETIC PROPERTIES AND ELECTRONIC STRUCTURE

As explained above, in this paper we are interested in the theoretical limits to spin-injection efficiency from MnGaAs and MnInAs. Therefore, it suffices to study the electronic structure of the above-defined ordered ferromagnetic phase of these materials. This is because disorder effects (e.g., alloy disorder, Mn clustering, MnAs precipitation, etc.), as well as the limited stability of the ferromagnetic phase, will clearly only serve to impede spin-polarized transport in these materials.

Our calculations show that the local magnetic moment of the Mn atom is $\sim 4.1\mu_b$, where μ_b is the Bohr magneton, for both MnGaAs and MnInAs. This value is in good agreement with previous calculations.^{16,19} Due to localization of spin-polarized charge around the Mn atom, this value is slightly larger than the global magnetic moment per supercell, which is $4\mu_b$. The latter value is in agreement with the magnetic moment of $5\mu_b$ for the free Mn atom being reduced to $4\mu_b$ in the lattice because the Mn impurity acts as an acceptor.

Having established that our calculation produces the correct magnetic properties, we now turn to assessing the electronic structure. Calculated total density-of-states (DOS) curves for MnGaAs and MnInAs, as well as those of the hypothetical zinc-blende MnAs phase, are shown in Fig. 1. It is readily observed that the zinc-blende MnAs is indeed half metallic, in agreement with previous studies.^{4,5} However, the DMSs are *not* strictly half metallic. The DOS of both majority and minority spins feature a similar band gap.²⁰ The Fermi-level position indicates that both DMSs are in fact p -type semiconductors with the Mn acting as an acceptor ion, in agreement with experiment.⁶ By integrating the DOS from the Fermi level to the valence-band maximum, we find that the hole density is $\sim 10^{21}$ cm⁻³. This value is at the upper end of the experimentally reported range of $\sim 10^{20}$ cm⁻³– $\sim 10^{21}$ cm⁻³ holes for MnGaAs samples of

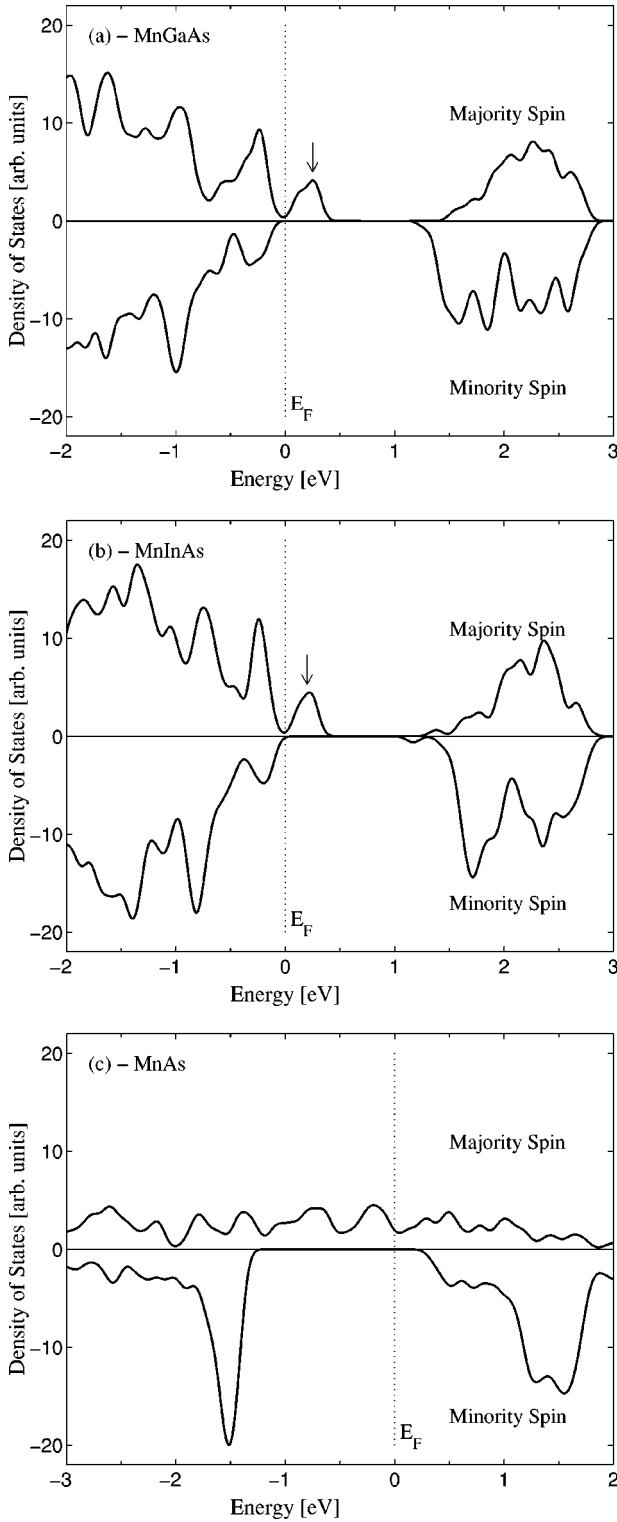


FIG. 1. Density-of-state curves for: (a) $\text{Mn}_{0.063}\text{Ga}_{0.937}\text{As}$, (b) $\text{Mn}_{0.063}\text{In}_{0.937}\text{As}$, and (c) zinc-blende MnAs . Arrows in (a) and (b) denote portion of states with potential for spin-polarized hole injection.

similar Mn concentration.⁶ The actual hole concentration can easily be lower due to compensating defects, which are not taken into account in our calculation. This semiconducting nature of the DMS with an x of $1/16$ is in contrast with

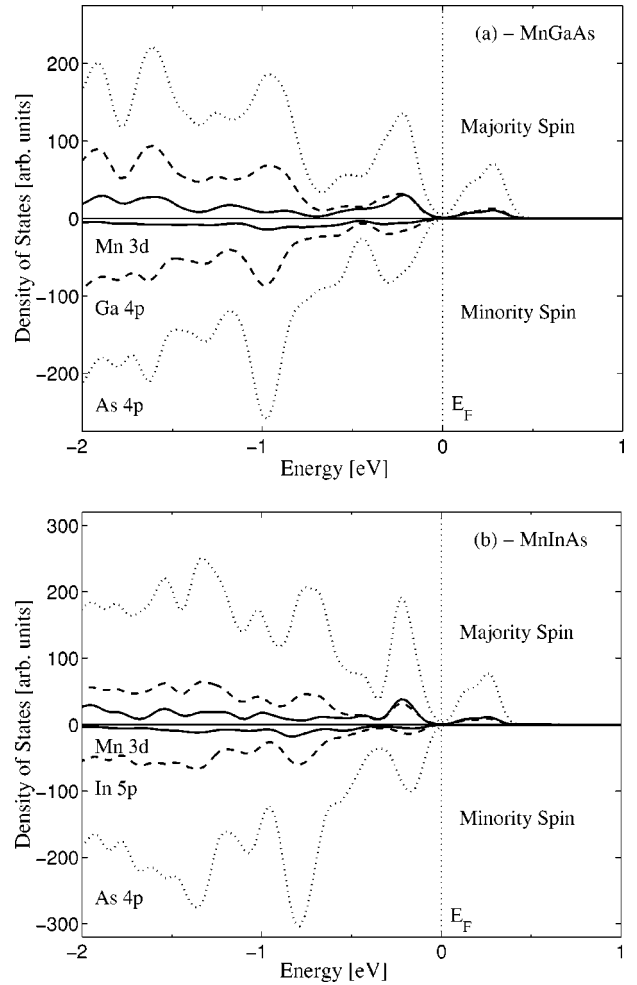


FIG. 2. Partial density-of-state curves for: (a) $\text{Mn}_{0.063}\text{Ga}_{0.937}\text{As}$, (b) $\text{Mn}_{0.063}\text{In}_{0.937}\text{As}$.

previous theoretical work,¹⁵ which found a strictly half-metallic band structure for $\text{Mn}_x\text{Ga}_{1-x}\text{As}$ with an x of $1/4$ and $1/8$, i.e., beyond the experimentally accessible range.

For the lower x value of $1/16$ that is studied here, we find that the ferromagnetic nature of the DMSs is manifested in a significant DOS just above the Fermi level (denoted by an arrow in Figs. 1(a) and 1(b), which appears in the majority spin DOS *alone*. This is, in principle, in agreement with the calculations of Park *et al.*¹⁶ on MnGaAs and of Akai¹⁹ on MnInAs , except for the more liberal definition of the term “half metal” by these authors. It is immediately obvious that any hope of obtaining holes with a well-defined spin from these DMS’s rests on this spin-polarized DOS near the valence band.

For understating the origin of the spin-polarized feature in the DOS curves, we calculated partial DOS curves near the top of the valence band for MnGaAs (MnInAs). The $\text{As } 4p$, $\text{Ga } 4p$ ($\text{In } 5p$), and $\text{Mn } 3d$ contributions to the DOS are shown in Fig. 2 (the partial DOS of all other orbitals was found to be negligible in the pertinent energy range). It is readily apparent that the $\text{Mn } 3d$ states hybridize strongly with $\text{As } 4p$ states, and to a much lesser extent with $\text{Ga } 4p$ ($\text{In } 5p$) states. The situation is similar to that encountered in

GaAs (InAs), where the top of the valence band is dominated by As $4p$ states.^{9,21} However, for the spin-up states the Mn $3d$ states contribute roughly as much as the original cation states, even though the Mn concentration is much lower than the Ga (In) one.

Figures 1 and 2 show that the electronic structures of $\text{Mn}_x\text{Ga}_{1-x}\text{As}$ and $\text{Mn}_x\text{In}_{1-x}\text{As}$ with $x = 1/16$ is an intermediate case between the limit of an isolated Mn atom in GaAs (InAs) on the one hand, and the limit of the zinc-blende MnAs phase on the other hand. The Mn content is clearly too large to consider each Mn atom as an isolated impurity. Indeed, a localized spin-polarized defect state situated ~ 0.1 eV above the valence-band maximum (VBM) (Ref. 22) is expected for an isolated impurity, whereas here the impurity-related feature is broad (~ 0.5 eV in width), due to orbital hybridization. However, while the Mn concentration does result in significant band splitting (see below), the hybridization, and therefore the split are too small to completely wipe out the majority-spin band gap. This is because there is at least one cation site containing Ga between two sites containing Mn, which impedes the hybridization.

In order to assess how efficient spin-polarized transport in these materials can be, we must consider the possible transport mechanism. Is it closer to the isolated impurity limit, where transport may be a free-hole mediated Ruderman-Kittel-Kasuya-Yosida (RKKY) mechanism,²³ or closer to the MnAs limit [as is MnGaAs with, e.g., $x = 1/2$ (Ref. 15)], where a band with a significant d character is formed?⁴

To answer this question, we calculated the band-structure diagrams for MnGaAs and MnInAs. These are given in Fig. 3, plotted for several high-symmetry directions in the Brillouin zone. Note that in light of our choice of a bcc supercell, the Brillouin zone must correspond to a bcc real-space lattice, even though the local atomic configuration is that of a slightly perturbed zinc-blende lattice. It is readily apparent that for both DMSs, the above-discussed spin-polarized feature in the majority-spin DOS is actually a distinct *band* of spin-polarized holes. The VBM of the majority spin is ~ 0.5 eV above that of the minority spin. Both VBMs are at the Γ point so that the band gaps for both spins are direct.

Our theoretical prediction of a split valence band is in qualitative agreement with experiment.²⁴ Quantitatively, however, experiment finds a smaller split, of the order of ~ 0.1 eV (Ref. 24). Because the samples used in experiments had a degree of disorder, the experimentally found splittings must be smaller than the value expected for the ideally ordered case studied here. Conversely, our calculated value is likely to overestimate the splitting. First, the local-spin-density approximation is known to overestimate Mn-related band splittings.²⁵ Second, spin-orbit coupling, which was not included in our calculations, may further reduce the band splitting. For the ideal case studied here, the combination of theory and experiment therefore provides an upper and lower bound, respectively, for the width of the spin-polarized energy range at the VBM.

Several bands with different effective masses are apparent around the Γ point of the majority-spin diagrams. By fitting these bands to a parabola around the Γ point, we find that the lighter holes have an effective mass of $0.1m_0$ and $0.05m_0$ for

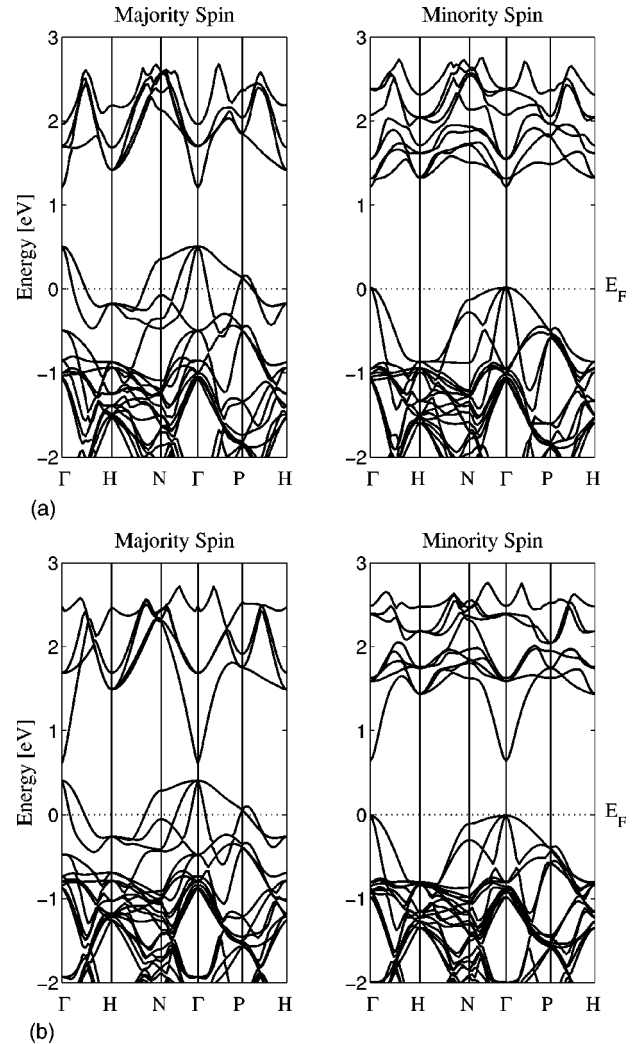


FIG. 3. Band-structure diagrams for: (a) $\text{Mn}_{0.063}\text{Ga}_{0.937}\text{As}$, (b) $\text{Mn}_{0.063}\text{In}_{0.937}\text{As}$.

MnGaAs and MnInAs , respectively, where m_0 is the electron rest mass. These numbers are of the same order of magnitude as the light hole mass in GaAs and InAs,²⁶ respectively, unequivocally indicating a very favorable situation for injection of spin-polarized holes into GaAs or InAs. We, therefore, find that spin-polarized transport in MnGaAs and MnInAs can be explained without resorting to the simple picture of a hole-providing isolated Mn impurity resulting in an RKKY-like mechanism. This is in agreement with a similar conclusion by Akai,¹⁹ obtained from different arguments.

For practical realization of this promising spin-injection potential, one must place the Fermi level such that injection takes place solely from the relatively narrow energy range between the minority-spin VBM and the majority-spin VBM. If this condition is fulfilled, then although neither MnInAs nor MnGaAs are half metallic, both can be considered as “locally half metallic,” in the sense that the holes in the energy range relevant for injection will be part of a continuous energy band with a well-defined spin.

In practice, the position of the Fermi level is determined by “unintentional doping” of defects and residual impurities. For example, such “unintentional doping” often results in

MnInAs that is n type, rather than p type.¹⁸ We, therefore, propose that a possible key to improving the spin-injection efficiency is careful control of the position of the Fermi level, e.g., by adding a different donor or acceptor species (in trace amounts, such that the band structure is not affected). We also stress that particular attention must be paid to appropriate design of the interface, where the Fermi-level position may be significantly altered due to interface states.²⁷ Such improvement of efficiency may, however, involve an important caveat. As noted above, our study pertains to the ferromagnetic phase only, but pushing the Fermi level upwards may result in a reduced stability of this phase.¹⁹ This may indicate a practical tradeoff between the degree of spin polarization and the Curie temperature.

It is also important to note that the practical attainment of “pure” bandlike transport also depends on the degree of order in the material, with hopping conductivity increasing in significance at the expense of bandlike transport with increasing disorder.²⁸ Indeed, the experimentally observed loss of metallic behavior at high Mn concentrations²⁹ may be attributed to an increasing disorder in the sample. As these effects are strongly growth and sample dependent and do not affect our discussion of the ultimate performance limits, they are not pursued further here.

V. CONCLUSIONS

In conclusion, we have used density-functional-theory-based calculations to elucidate the electronic structure of MnGaAs and MnInAs with an experimentally realistic Mn content. We find that both materials possess a band of well-defined spin. This band is derived from hybridization of Mn $3d$ and As $4p$ states. By stringent material and device design that places the Fermi-level position close to the maximum of this band, and assuming a sufficiently high degree of order and a sufficiently low temperature, MnGaAs and MnInAs can indeed be used as an ideal source of spin-polarized holes that is compatible with the existing III-V technology.

ACKNOWLEDGMENTS

This work was supported in part by the National Science Foundation, the MRSEC program of the National Science Foundation under Award No. DMR-9809364, and the Minnesota Supercomputing Institute. We would like to thank Serdar Ögüt, Chris Palmström, and Paul A. Crowell for illuminating discussions.

-
- ¹S. Datta and B. Das, *Appl. Phys. Lett.* **56**, 665 (1990).
²G. Prinz, *Science* **282**, 1660 (1998).
³G. Burkard, D. Loss, and D. P. DiVincenzo, *Phys. Rev. B* **59**, 2070 (1999).
⁴M. Shirai, T. Ogawa, I. Kitagawa, and N. Suzuki, *J. Magn. Magn. Mater.* **177-181**, 1383 (1998).
⁵S. Sanvito and N. A. Hill, *Phys. Rev. B* **62**, 15 553 (2000).
⁶H. Ohno, *Science* **281**, 951 (1998), and references therein.
⁷B. Beschoten, P. A. Crowell, I. Malajovich, D. D. Awschalom, F. Matsukura, A. Shen, and H. Ohno, *Phys. Rev. Lett.* **83**, 3073 (1999).
⁸Y. Ohno, D. K. Young, B. Beschoten, F. Matsukura, H. Ohno, and D. D. Awschalom, *Nature (London)* **402**, 790 (1999).
⁹J. R. Chelikowsky and M. L. Cohen, in *Handbook on Semiconductors*, 2nd ed., edited by T. S. Moss (Elsevier, Amsterdam, 1992); W. E. Pickett, *Comput. Phys. Rep.* **9**, 115 (1989).
¹⁰J. Perdew and Y. Wang, *Phys. Rev. B* **45**, 13 244 (1992).
¹¹N. Troullier and J. L. Martins, *Phys. Rev. B* **43**, 1993 (1991).
¹²L. Kleinman and D. M. Bylander, *Phys. Rev. Lett.* **48**, 1425 (1982).
¹³H. J. Monkhorst and J. D. Pack, *Phys. Rev. B* **13**, 5188 (1976).
¹⁴D. F. Shanno and K.-H. Phua, *Math. Program.* **14**, 149 (1978).
¹⁵T. Ogawa, M. Shirai, N. Suzuki, and I. Kitagawa, *J. Magn. Magn. Mater.* **196-197**, 428 (1999).
¹⁶J. H. Park, S. K. Kwon, and B. I. Min, *Physica B* **281-282**, 703 (2000).
¹⁷R. Shioda, K. Ando, T. Hayashi, and M. Tanaka, *Phys. Rev. B* **58**, 1100 (1998).
¹⁸Y. L. Soo, S. W. Huang, Z. H. Ming, Y. H. Kao, H. Munekeata, and L. L. Chang, *Phys. Rev. B* **53**, 4905 (1996).
¹⁹H. Akai, *Phys. Rev. Lett.* **81**, 3002 (1998).
²⁰The underestimate of the bandgap is a well-known shortcoming of density-functional theory (see Ref. 9) that does not affect the accuracy of the valence-band results.
²¹J. C. Woicik, E. J. Nelson, T. Kendelwicz, P. Pianneta, M. Jain, L. Kronik, and J. R. Chelikowsky, *Phys. Rev. B* **63**, R041403 (2001).
²²M. Linnarsson, E. Janzén, B. Monemar, M. Kleverman, and A. Thilderkvist, *Phys. Rev. B* **55**, 6938 (1997).
²³T. Dietl, A. Haury, and Y. Merle d’Aubigné, *Phys. Rev. B* **55**, R3347 (1997).
²⁴J. Szczytko, W. Mac, A. Twardowski, F. Matsukura, and H. Ohno, *Phys. Rev. B* **59**, 12 935 (1999), and references therein.
²⁵S.-H. Wei and A. Zunger, *Phys. Rev. B* **48**, 6111 (1993).
²⁶*Semiconductors: Group IV and III-V compounds*, Data in Science and Technology Series, edited by O. Madelung (Springer-Verlag, Berlin, 1991).
²⁷W. Mönch, *Semiconductor Surfaces and Interfaces* (Springer-Verlag, Berlin, 1993).
²⁸N. Mott, *Conduction in Non-Crystalline Materials* (Oxford University Press, Oxford, 1987).
²⁹A. Oiwa, S. Katsumoto, A. Endo, M. Hirasawa, Y. Iye, H. Ohno, F. Matsukura, A. Shen, and Y. Sugawara, *Solid State Commun.* **103**, 209 (1997).